

GSC 04263-02166 IS A LOW-AMPLITUDE MULTI-PERIODIC DELTA SCUTI VARIABLE

LLOYD, CHRISTOPHER¹; ÖĞMEN, YENAL^{2,6}; KOFF, ROBERT A.^{3,6}; COOK, LEWIS M.^{4,6};
PICKARD, ROGER^{5,7}

1) Department of Physics and Astronomy, University of Sussex, Brighton, BN1 9QH, UK C.Lloyd@sussex.ac.uk

2) CBA Cyprus, Green Island Observatory, Gecitkale, North Cyprus yenalogmen@yahoo.com

3) CBA Colorado, Antelope Hills Observatory, 980 Antelope Drive West, Bennett, CO 80102, USA

4) CBA Concord, 1730 Helix Ct., Concord, CA 94518, USA

5) 3 The Birches, Shobdon, Leominster, Herefordshire, HR6 9NG, UK

6) American Association of Variable Star Observers, 49 Bay State Rd. Cambridge, MA 02138, USA

7) The British Astronomical Association, Variable Star Section (BAA VSS), Burlington House, Piccadilly, London, W1J 0DU, UK

Abstract: GSC 04263-02166 is found to be a low-amplitude δ Scuti variable with at least four frequencies. The dominant one lies at $f_1 = 22.0156(9)$ with the other most likely frequencies being 17.9703(14), 15.7615(20) and 22.9363(22) cd^{-1} . The full amplitudes are 8.2(4), 5.6(4), 3.8(4) and 3.5(4) millimagnitudes respectively and these four frequencies account for about 82% of the power in the variation. Any remaining frequencies lie below the noise limit of ~ 1.4 mmag. The frequency ratios of $f_2/f_1 = 0.816$ and $f_3/f_2 = 0.877$ suggest that the star is a non-radial pulsator.

1 Introduction

The δ Scuti stars are the most common variables of spectral types A - mid-F type and occur on or above the main sequence where the instability strip crosses it. They have dominant frequencies in the range $\sim 5 - 30 \text{ cd}^{-1}$ and can pulsate in both radial and/or non-radial modes and combination frequencies. Their value as probes of stellar structure has long been recognised and this was largely responsible for the development of asteroseismology. About 30% of δ Sct stars are low-amplitude variables with a range of < 0.05 magnitudes (from ground-based data) and there is a tail of high-amplitude δ Sct stars (HADS) with amplitudes > 0.3 magnitudes, where radial modes tend to dominate (Chang et al., 2013). Due to their particular properties the HADS stars are often treated as a separate group but Balona (2016) has suggested that they are simply the high amplitude tail of the δ Sct distribution. The other related variables that inhabit this part of the HR diagram are the SX Phoenicis stars, which are low-metallicity analogues of the δ Scuti stars and the γ Doradus stars, which again are low-amplitude variables with periods ~ 1 day. Hybrid δ Sct/ γ Dor objects have been found (see Poretti et al., 2011; Sánchez Arias et al., 2017, and references therein) but Balona et al. (2015) finds that all δ Sct stars in a *Kepler* sample contain low frequency $\sim 1 - 5 \text{ cd}^{-1}$ components in the γ Dor frequency range which raises doubts about the hybrid class. The implication of this is

Table 1: List of equipment used.

| Observer | Telescope | CCD | Filter |
|----------|---------------------------------|--------------------------|---------------------|
| Cook | Prime Focus 0.74-m reflector | SBIG STF8300M | Clear |
| Koff | Meade 0.25-m LX200 SCT | Apogee Alta U-47 | Clear + IR block |
| Öğmen | Meade 0.35-m LX200R SCT | SBIG ST8XME | Clear |
| Pickard | Meade 0.35m LX200 SCT | Starlight Xpress SXVF-H9 | V |

that the δ Sct and γ Dor stars are physically different groups with all δ Sct stars containing low-frequency components and at least some γ Dor stars containing high-frequency components.

GSC 04263-02166 (UCAC4 751-072304) was found to be variable by Öğmen (2016) during observations of the field containing two other recently discovered variables. These are a 15th magnitude W UMa system UCAC4 751-072394 = 2MASS J22092168+6006483 (Banfi et al., 2016) and a slightly brighter EA binary UCAC4 751-072412 = 2MASS J22092980+6003263 (Papini et al., 2016). Observations of both these systems will be reported elsewhere.

2 Observations

The observations were made from four sites spanning the longitude range of approximately 2 hours East to 8 hours West using a variety of telescopes and CCD detectors as described in Table 1. All the images were dark-subtracted and flat-fielded before being analysed using commercially available differential aperture photometry software against a comparison star sequence. Each observer used a different ensemble of comparison stars depending on the field of view of their equipment or other constraints. The comparisons were drawn from the sequence given in Table 2 which lists suitable stars of modest colour and with no sign of variability at this level. The data are taken from the VizieR listing of the UCAC4 Catalogue (Zacharias et al., 2012) and AAVSO Photometric All Sky Survey (APASS Henden et al. (2016)) which gives Johnson BV and Sloan Digital Sky Survey (SDSS) g' , r' and i' magnitudes.

In total over 50 hours of observations were made on 11 nights over a period of 22 days as detailed in Table 3. Runs of more than 5 hours were taken on over half the nights while the remaining nights had shorter or broken runs. Visual inspection of the data shows a clear variation of ~ 0.02 magnitudes on a time scale of ~ 1 hour, but the amplitude is variable suggesting multiple frequencies. The raw data are all available from the AAVSO database.

Table 2: Comparison star sequence. Positional and photometric data are given for the variable (first line) and then for suitable comparison stars in order of increasing distance from the variable up to 6.6 arc minutes. The data are taken from the VizieR listing of the UCAC4 and APASS Catalogues

| RA | Dec | UCAC4 | B | V | g' | r' | i' | $B - V$ |
|--------------|--------------|------------|--------|--------|--------|--------|--------|---------|
| 22 08 56.581 | +60 09 40.02 | 751-072304 | 13.725 | 12.988 | 13.322 | 12.791 | 12.491 | 0.737 |
| 22 08 54.978 | +60 10 06.21 | 751-072297 | 16.442 | 15.786 | 16.078 | 15.421 | 15.172 | 0.656 |
| 22 08 50.453 | +60 10 20.06 | 751-072281 | 14.025 | 13.421 | 13.700 | 13.328 | 13.113 | 0.604 |
| 22 09 06.172 | +60 09 45.94 | 751-072338 | 14.009 | 13.231 | 13.594 | 13.035 | 12.755 | 0.778 |
| 22 08 54.111 | +60 07 50.17 | 751-072295 | 11.163 | 10.559 | 10.854 | 10.439 | 10.180 | 0.604 |
| 22 09 11.337 | +60 08 43.86 | 751-072356 | 16.158 | 15.304 | 15.912 | 15.093 | 14.470 | 0.854 |
| 22 09 13.781 | +60 09 05.62 | 751-072364 | 16.657 | 15.761 | 16.116 | 15.450 | 15.003 | 0.896 |
| 22 09 17.212 | +60 09 08.72 | 751-072380 | 15.893 | 15.020 | 15.458 | 14.743 | 14.244 | 0.873 |
| 22 08 35.139 | +60 08 55.42 | 751-072232 | 15.199 | 14.500 | 14.810 | | | 0.699 |
| 22 08 58.851 | +60 12 27.35 | 752-071854 | 17.548 | 16.777 | | | | 0.771 |
| 22 09 02.774 | +60 12 31.05 | 752-071863 | 16.748 | 15.914 | 16.329 | 15.567 | 15.031 | 0.834 |
| 22 08 55.869 | +60 06 17.36 | 751-072302 | 16.600 | 15.874 | 16.307 | 15.368 | 14.965 | 0.726 |
| 22 09 04.274 | +60 05 43.69 | 751-072331 | 16.210 | 15.532 | | | | 0.678 |
| 22 08 42.304 | +60 05 36.85 | 751-072254 | 12.951 | 12.281 | 12.575 | 12.131 | 11.882 | 0.670 |
| 22 08 35.443 | +60 13 30.18 | 752-071793 | 17.235 | 16.621 | 16.875 | 16.071 | | 0.614 |
| 22 09 19.241 | +60 13 45.41 | 752-071906 | 14.546 | 13.767 | 14.125 | 13.541 | 13.183 | 0.779 |
| 22 08 54.484 | +60 14 39.59 | 752-071844 | 15.200 | 14.448 | 14.797 | 14.215 | 13.970 | 0.752 |
| 22 08 32.317 | +60 14 17.59 | 752-071784 | 16.089 | 15.483 | | | | 0.606 |
| 22 09 07.718 | +60 04 17.96 | 751-072342 | 16.282 | 15.439 | 15.853 | 15.201 | 14.837 | 0.843 |
| 22 09 40.335 | +60 12 00.71 | 752-071959 | 14.029 | 13.426 | 13.712 | 13.358 | 13.155 | 0.603 |
| 22 09 43.795 | +60 07 50.99 | 751-072473 | 13.842 | 13.257 | 13.518 | 13.165 | 12.971 | 0.585 |
| 22 09 05.478 | +60 03 27.85 | 751-072335 | 16.775 | 15.969 | | | | 0.806 |
| 22 08 38.083 | +60 15 51.44 | 752-071803 | 13.199 | 12.462 | 12.802 | 12.284 | 12.028 | 0.737 |

Table 3: Observation log.

| UT Date | JD range | Duration (hours) | Band | Observer |
|-------------|--------------------|------------------|------|----------|
| 2016 Sep 30 | 2457662.220 - .428 | 5.0 | CV | Öğmen |
| 2016 Oct 05 | 2457667.277 - .434 | 3.8 | V | Pickard |
| 2016 Oct 06 | 2457667.629 - .701 | 1.7 | CV | Cook |
| 2016 Oct 06 | 2457667.816 - .885 | 1.6 | CV | Cook |
| 2016 Oct 07 | 2457668.617 - .661 | 1.1 | CV | Cook |
| 2016 Oct 07 | 2457668.726 - .904 | 4.3 | CV | Cook |
| 2016 Oct 08 | 2457669.580 - .849 | 6.5 | CV | Koff |
| 2016 Oct 08 | 2457670.195 - .403 | 5.0 | CV | Öğmen |
| 2016 Oct 09 | 2457670.722 - .901 | 4.3 | CV | Cook |
| 2016 Oct 10 | 2457672.305 - .392 | 2.1 | V | Pickard |
| 2016 Oct 14 | 2457676.197 - .405 | 5.0 | CV | Öğmen |
| 2016 Oct 21 | 2457682.559 - .801 | 5.8 | CV | Koff |
| 2016 Oct 22 | 2457684.187 - .395 | 5.0 | CV | Öğmen |

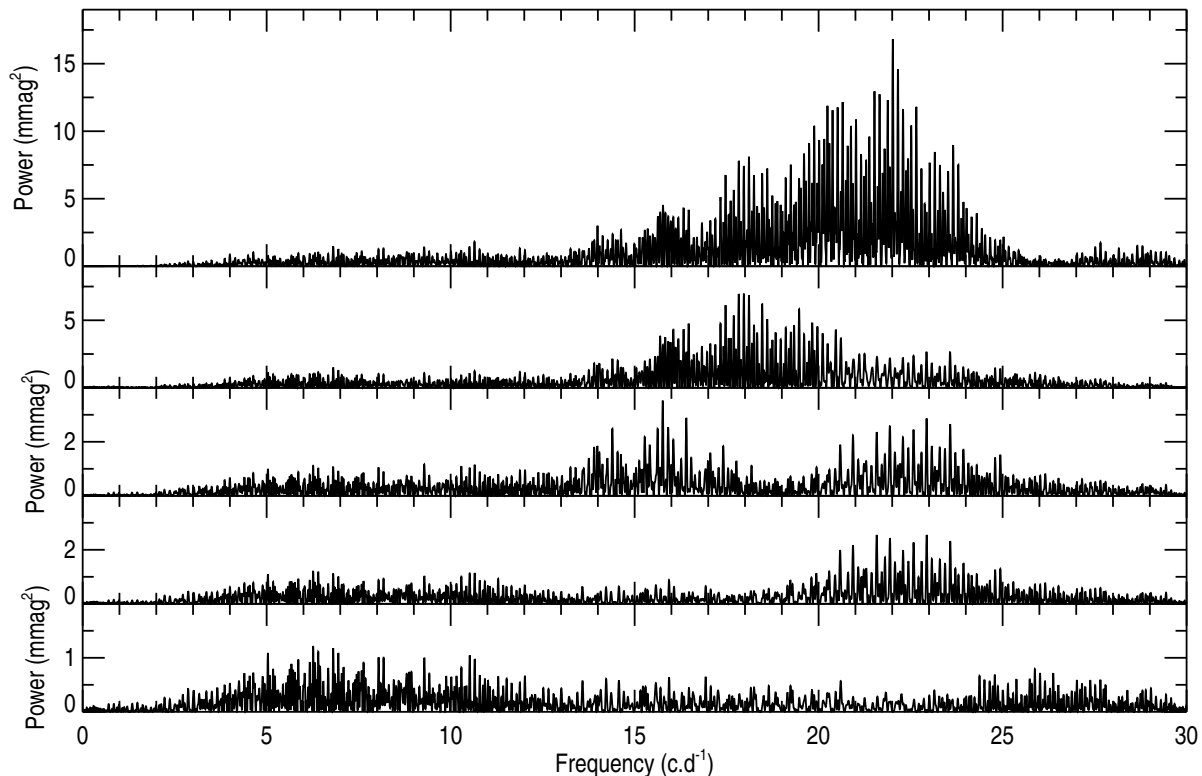


Figure 1: The DFT power spectrum of the data prior to the removal of each frequency. The y-axis is in units of millimagnitudes² and each panel is multiplied by a relative scale factor of 1, 1, 2, 2, 4 respectively in order to bring out the weaker details. The maximum power above 30 c d^{-1} is $\sim 0.2 \text{ mmag}^2$.

3 Frequency Analysis

Due to the inhomogeneous nature of the data they were first smoothed to some extent by a median filter to produce independent points with approximately the same uncertainty, ~ 0.0015 magnitudes. Also, because the measurements were with different equipment, different comparison stars and different V and CV systems it was necessary to remove the mean of each run. The data were also detrended to remove potential differential extinction effects, and while these were mostly insignificant this will remove any potential variation on the scale of a few cycles per day.

The data were processed through both a simple Discrete Fourier Transform (DFT) and a Lomb-Scargle periodogram (Lomb, 1976; Scargle, 1982), and in terms of the frequencies identified the results were the same. As each frequency was found it and the preceding ones were removed by a simultaneous multi-frequency least-squares sine fit and the residuals were then searched for any remaining frequencies, and the process repeated until the noise level was reached. Ultimately four frequencies were found (as given in Table 4) although the value of the fourth is not certain.

The results of the frequency search are displayed in Figure 1 which shows the DFT power spectrum of the data prior to the removal of each frequency. The bottom panel

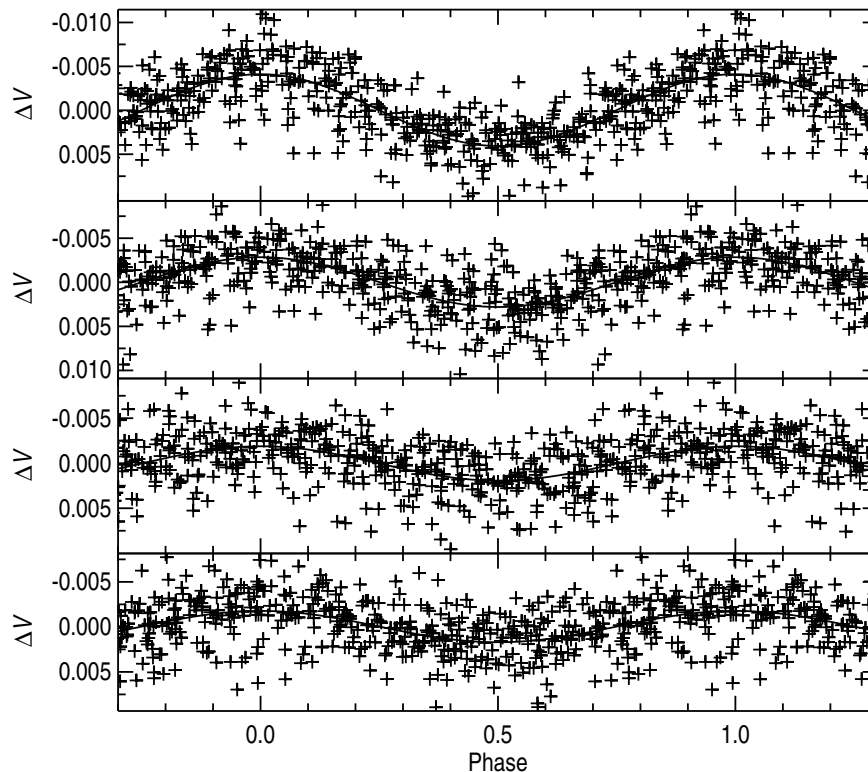


Figure 2: The phase diagram of the four identified frequencies plotted with the same vertical scale. The fourth frequency is included to illustrate the level of this variation.

shows the remaining power after the four frequencies have been removed. The peak noise level occurs at $\sim 6 \text{ c d}^{-1}$ and corresponds to an amplitude of 2.2 mmag, and most of the remaining power appears in this frequency range. Where frequencies have been removed the noise level corresponds to an amplitude of $\sim 1.8 \text{ mmag}$ and for frequencies above 30 c d^{-1} , in the realm of $2f_i$, the noise level is $< 1 \text{ mmag}$.

While the dominant frequency, f_1 , is clear it has to be said that f_2 is less obvious and has two uncomfortably large aliases. These lie at $f = 17.829$ and 18.108 c d^{-1} but different subsets of the data with different resampling regimes tend to confirm that f_2 is correctly identified as it always leads to the smallest residuals in the four-frequency fit and the cleanest periodogram in $10 - 30 \text{ c d}^{-1}$ frequency range. The value of f_4 is not clear as there is a viable alternative at $f = 21.578 \text{ c d}^{-1}$, and other aliases with similar amplitudes, but which is chosen makes very little difference to the final residuals. Also the largest feature in this frequency range in the bottom panel of Figure 1 corresponds to only a minor feature in the panel above. The fourth frequency has only been included as an illustration of the variation at this level.

Because the data were detrended nothing can be said about low frequencies, those below the lengths of the data runs, $\sim 4 \text{ c d}^{-1}$, and indeed there is nothing to see, but features in the $\sim 5 - 10 \text{ c d}^{-1}$ range do pose a difficulty. They are nominally sampled about twice per (long) observing run so they could conceivably reflect real power in this

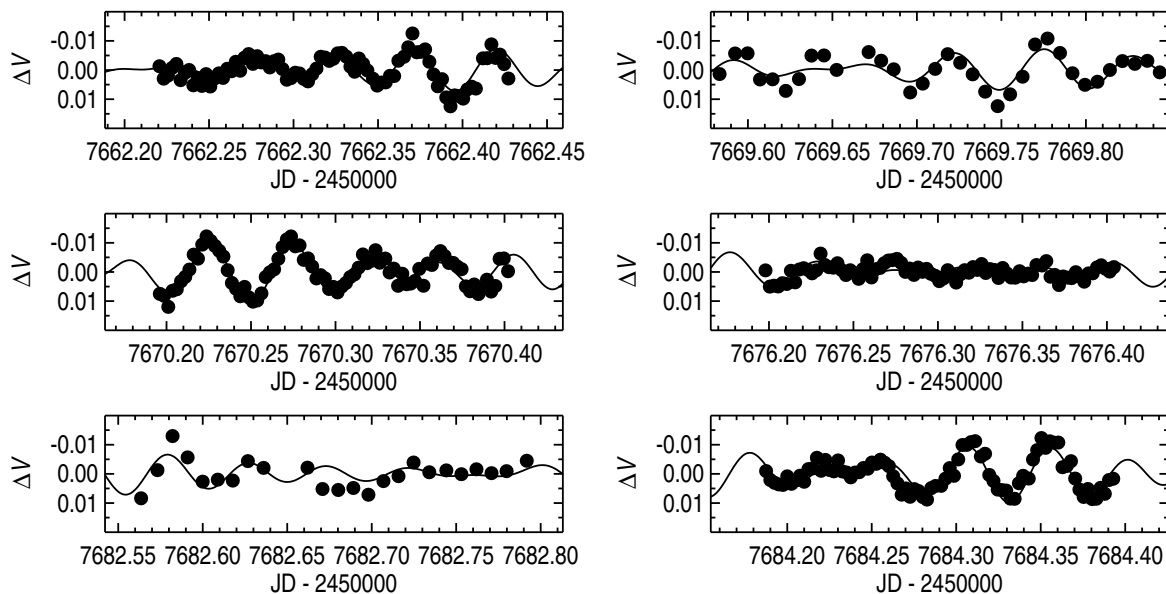


Figure 3: The six longest runs with the the four-frequency fit superimposed. The interaction between the different frequencies can be clearly seen with the amplitude increasing or decreasing through runs. On one run the variation almost ceases altogether but the dominant frequency can still be recovered. However, the systematic errors in some of the fits are clear. The error bars are approximately the same size as the symbols and have been omitted for clarity.

Table 4: Frequencies and full amplitudes of the four frequencies found in the data. The frequency ratios are calculated so as to resolve to < 1 .

| i | f_i c d^{-1} (error) | Amplitude (error) | f_i/f_1 | f_i/f_2 | f_i/f_3 | f_i/f_4 |
|---|---------------------------------|-------------------|-----------|-----------|-----------|-----------|
| 1 | 22.0156(9) | 0.0082(4) | 1 | | | 0.960 |
| 2 | 17.9703(14) | 0.0056(4) | 0.816 | 1 | | 0.785 |
| 3 | 15.7615(20) | 0.0038(4) | 0.716 | 0.877 | 1 | 0.687 |
| 4 | 22.9363(22) | 0.0035(4) | | | | 1 |

frequency range as seen in the hybrid δ Sct/ γ Dor systems and *Kepler* data. However, until this frequency range can be properly explored it is not clear if these features are real or artefacts related to differential extinction issues.

The standard deviation of the residuals from the four-frequency fit is 2.7 mmag, however, this is significantly larger than the estimated errors and indicates that either the fit is poorer than expected or that the errors are underestimated. Given that the errors are determined from the variance of the data this seems unlikely. Also the fit to the data in Figure 3 does show some systematic differences so it seems more likely that there is either additional signal in the data that has not been removed or that signal has been introduced through detrending the data.

It has been recognised for some decades (e.g., Breger, 1980a) that the frequencies of radial pulsation modes have particular ratios which have been refined both observationally and theoretically, and a dependence on mass, temperature and metallicity has been

established (see e.g., Suárez et al., 2007). The frequency ratio of the fundamental to the first overtone lies in a narrow range of 0.774 ± 0.007 and from the ratios given in Table 4 none of them are consistent with this, and the closest involves the weakest frequency. For the most reliable frequencies the ratios are $f_2/f_1 = 0.816$, $f_3/f_1 = 0.715$ and $f_3/f_2 = 0.877$ which are not consistent with the radial-mode ratio. In stars with radial modes and many frequencies the bulk of these are combination frequencies made up of the different radial modes. In this star none of the frequencies are simple combinations of the others so on both counts the star most likely a non-radial pulsator.

The ratio of f_2/f_1 is close to the ratio of the first and second radial overtone modes (see e.g., Breger, 1979, 1980b; Bono et al., 1997) but that would imply that the dominant frequency f_1 , is the radial second overtone, that f_2 is the first overtone and that the fundamental would be close to $f \sim 13.9 \text{ cd}^{-1}$. While there are features around this frequency they are weak. Also, f_3 and f_4 would have to be considered as non-radial so again it is most likely that the star is a non-radial pulsator.

4 Intrinsic colours and luminosity

The observed magnitudes of GSC 04263-02166 are given on the first line of Table 2 but these are limited to B , V and g' , r' and i' from the UBV and SDSS prime systems. Using the transformations of Smith et al. (2002) it is possible to reconstruct BVR_cI_c from the Sloan magnitudes as, $B = 13.74$, $V = 13.00$, $R_c = 12.57$ and $I_c = 12.07$ and colours of $B - V = 0.742$, $V - R_c = 0.423$ and $R_c - I_c = 0.510$. The difference from the observed B and V magnitudes and colour is ~ 0.01 which suggests that the other colours should be equally reliable. Using the standard reddening model (see e.g., Schlafly & Finkbeiner, 2011, and references therein) for $R_V = 3.1$ and the intrinsic colours of main sequence stars from Pecaut & Mamajek (2013) gives an unreddened $(B - V)_0 = 0.28(3)$, corresponding to a star with a spectral type of A8 – F0. Combined with the observed $B - V = 0.74$ this gives the reddening $E_{B-V} = 0.46$ and with $R_V = 3.1$ then $A_V = 1.4$ magnitudes.

In addition to the BV and Sloan photometry the 2MASS catalogue (Skrutskie et al., 2006) gives $J = 11.41(2)$, $H = 11.18(3)$ and $K_s = 11.06(3)$ which provide another route to the reddening. From the observed colours of $J - H = 0.23(3)$ and $H - K_s = 0.12(4)$ and the calibration of Straižys & Lazauskaitė (2009) with their reddening vector, $E_{(J-H)}/E_{(H-K_s)} = 2.0$ leads to dereddened colours, assuming a main sequence star, of $(J - H)_0 = 0.08(3)$ and $(H - K_s)_0 = 0.04(4)$. These correspond to a spectral type of A7 – F2 (see Pecaut & Mamajek, 2013) and are very similar to the earlier result.

GSC 04263-02166 lies at galactic coordinates of $l = 104^\circ$, $b = +3^\circ$ so significant reddening is to be expected. The WEBDA Catalogue ¹ list two open clusters within two degrees of this position, ASCC 117 and ASCC 118, which both have reddening $E_{B-V} = 0.30$ and lie at distances of 1200 and 900 parsec respectively. The total reddening in the 5 arc minutes around this direction ² is $E_{B-V} = 1.1 \pm 0.1$ which provides an upper limit

¹WEBDA A site Devoted to Stellar Clusters in the Galaxy and the Magellanic Clouds
<https://www.univie.ac.at/webda/interrogation.html>

²NASA/IPAC Infrared Science Archive Galactic Dust Reddening and Extinction Service
<http://irsa.ipac.caltech.edu/applications/DUST/>

to the extinction (Schlafly & Finkbeiner, 2011).

From the cluster distances and reddening, and with $R_V = 3.1$ the linear rate of extinction is approximately 1.0 magnitudes kpc^{-1} , and if the extinction to the star is $A_V = 1.4$ magnitudes then the distance is ~ 1.4 kpc, with the obvious caveats. With $V = 13.0$ then the absolute magnitude, $M_V = 0.9$ which is ~ 1.6 magnitudes above the main sequence for an F0 star (Pecaut & Mamajek, 2013). These values translate to $\log(L/L_\odot) \sim 1.5$ and $\log(T_e) = 3.86$ which lies in the more luminous third of the δ Sct population (see e.g., Balona, 2016).

5 Discussion

While both the frequency analysis and the luminosity and intrinsic colours suggest that GSC 04263-02166 is a galactic disc δ Sct variable there are two rather different measurements of the proper motion to consider. In the latest offering from the UCAC stable the UCAC5 Catalogue (Zacharias et al., 2017) give the proper motion as $\mu_\alpha = -8.3(1.4)$ and $\mu_\delta = -5.0(1.4)$ mas yr^{-1} , similar to earlier versions of the catalogue. At a distance of 1.4 kpc this translates to a transverse velocity, $V_T = 64(13)$ km s^{-1} , but this does not include any uncertainty in the distance. Such a velocity is suspiciously large for a disc star, particularly at $l = 104^\circ$ and raises the possibility that the star is either an SX Phe variable, or is much closer. If it is closer then it has to be less luminous, for example an sdB or cool white dwarf but these would be inconsistent with the observed $B - V$ and so can be ruled out. The second set of proper motions from the XPM Catalogue (Fedorov et al., 2011) gives two calibrations averaging at, $\mu_\alpha = 2$ and $\mu_\delta = -5$ mas yr^{-1} , which are barely significant. It seems that this question along with many others will have to wait for the full *Gaia* results.

6 Conclusions

Time series observations of the 13th magnitude star GSC 04263-02166 reveal that it is a low-amplitude δ Scuti variable with at least four frequencies. The dominant one lies at $f_1 = 22.0156(9)$ with the other most likely frequencies being $17.9703(14)$, $15.7615(20)$ and $22.9363(22)$ cd^{-1} with full amplitudes of $8.2(4)$, $5.6(4)$, $3.8(4)$ and $3.5(4)$ millimagnitudes respectively. The level and complexity of the variations are at the limit of what can be extracted from these data and the value of the fourth frequency is little more than a suggestion. The limited final fit to the data does hint at the possibility of further frequencies, perhaps in the $1 - 10$ cd^{-1} range. Any remaining frequencies lie below the noise limit of ~ 1.4 mmag. The frequency ratios suggest that the star is a non-radial pulsator. From the available photometry the reddening $E_{B-V} = 0.46$ and the intrinsic $(B - V)_0 = 0.28(3)$ corresponds to a star of spectral type A8 – F0. The star probably lies at ~ 1.4 kpc with $M_V = 0.9$ mag and is probably ~ 1.6 magnitudes above the main sequence.

Acknowledgements: The authors are pleased to acknowledge use of the VizieR and Simbad databases operated by the Centre de Données Astronomiques (University of Strasbourg), the VSX and APASS databases operated by the American Association of Variable Star Observers, and NASA’s Astrophysics Data System. This research has made use of the WEBDA database, operated at the Department of Theoretical Physics and Astrophysics of the Masaryk University and the NASA/IPAC Infrared Science Archive, which is operated by the Jet Propulsion Laboratory, California Institute of Technology, under contract with the National Aeronautics and Space Administration.

References

- Balona, L. A., Daszyńska-Daszkiewicz, J., & Pamyatnykh, A. A. 2015, MNRAS, 452, 3073 [2015MNRAS.452.3073B](#)
- Balona, L. A., 2016, MNRAS, 459, 1097 [2016MNRAS.459.1097B](#)
- Banfi, M., Marchini, A., Papini, R., Salvaggio, F., 2016, <https://www.aavso.org/vsx/index.php?view=detail.top&oid=473930>
- Bono, G., Caputo, F., Cassisi, S., et al. 1997, ApJ, 477, 346 [1997ApJ...477..346B](#)
- Breger, M. 1979, PASP, 91, 5 [1979PASP...91....5B](#)
- Breger, M. 1980a, Space Sci. Rev., 27, 361 [1980SSRv...27..361B](#)
- Breger, M. 1980b, ApJ, 237, 850 [1980ApJ...237..850B](#)
- Chang, S.-W., Protopapas, P., Kim, D.-W., & Byun, Y.-I. 2013, AJ, 145, 132, [2013AJ....145..132C](#)
- Cutri, R. M., Skrutskie, M. F., van Dyk, S., et al. 2003, VizieR Online Data Catalog, 2246, [2003yCat.2246....0C](#) (2MASS)
- Fedorov, P. N., Akhmetov, V. S., & Bobylev, V. V. 2011, MNRAS, 416, 403 [2011MNRAS.416..403F](#) VizieR [2003yCat.2246....0C](#) (XPM)
- Guzik, J. A., Bradley, P. A., Jackiewicz, J., et al. 2015, Astron. Rev., 11, 1 [2015AstRv..11....1G](#)
- Henden, A. A., Templeton, M., Terrell, D., et al. 2016, VizieR Online Data Catalog, 2336, [2016yCat.2336....0H](#) (APASS)
- Lomb, N. R. 1976, Ap&SS, 39, 447 [1976Ap&SS..39..447L](#)
- Öğmen, Y., 2016, <https://www.aavso.org/vsx/index.php?view=detail.top&oid=477108>
- Papini, R., Salvaggio, F., Marchini, A., Banfi, M., 2016, <https://www.aavso.org/vsx/index.php?view=detail.top&oid=473909>

- Pecaut, M. J., & Mamajek, E. E. 2013, ApJS, 208, 9 [2013ApJS..208....9P](#)
- Poretti, E., Rainer, M., Weiss, W. W., et al. 2011, A&A, 528, A147
[2011A&A...528A.147P](#)
- Sánchez Arias, J. P., Córscico, A. H., & Althaus, L. G. 2017, A&A, 597, A29
[2017A&A...597A..29S](#)
- Scargle, J. D. 1982, ApJ, 263, 835 [1982ApJ...263..835S](#)
- Schlafly, E. F., & Finkbeiner, D. P. 2011, ApJ, 737, 103 [2011ApJ...737..103S](#)
- Skrutskie, M. F., Cutri, R. M., Stiening, R., et al. 2006, AJ, 131, 1163
[2006AJ....131.1163S](#)
- Smith, J. A., Tucker, D. L., Kent, S., et al. 2002, AJ, 123, 2121 [2002AJ....123.2121S](#)
- Straižys, V., & Lazauskaitė, R. 2009, Baltic Astronomy, 18, 19 [2009BaltA..18...19S](#)
- Suárez, J. C., Garrido, R., & Moya, A. 2007, A&A, 474, 961 [2007A&A...474..961S](#)
- Watson, C., Henden, A. A., & Price, A. 2016, VizieR Online Data Catalog, 1,
[2016yCat....102027W](#) (VSX)
- Zacharias, N., Finch, C. T., Girard, T. M., et al. 2012, VizieR Online Data Catalog, 1322,
[2012yCat.1322....0Z](#) (UCAC4)
- Zacharias, N., Finch, C., & Frouard, J. 2017, VizieR Online Data Catalog, 1340,
[2017yCat.1340....0Z](#) (UCAC5)